

Visualization and Animation of Instrumentation Channel Effects on DFR Data Accuracy

A. P. Sakis Meliopoulos and George J. Cokkinides
 School of Electrical and Computer Engineering
 Georgia Institute of Technology
 Atlanta, Georgia 30332
 Sakis.meliopoulos@ece.gatech.edu

Abstract: Disturbance Fault Recorders collect data that are supposed to be exact replicas of the time waveforms in the electric power system. The voltages and currents of the electric power system are scaled via instrument transformers and other attenuators to voltages and currents that are compatible with analog to digital converter equipment. We refer to the instrument transformers, connecting control cables, attenuators, analog to digital converters, etc. as instrumentation channel. An ideal instrumentation channel will be one that produces at the output a waveform which is an exact scaled replica of the waveform at the high voltage power system. Unfortunately, instrumentation channels are not ideal but introduce errors and therefore the output waveform is not an exact scaled replica of the waveform. If the characteristics of the instrumentation channel are known, then the error introduced by the instrumentation channel can be computed. We present methods for the accurate evaluation of these errors. The results are illustrated in an animated fashion so that the user can identify the errors and the source of the errors. The inverse method provides the basis to correct these errors by appropriate processing. The importance of this work is the ability to improve the accuracy of the DFR data, i.e. the ability to reconstruct an almost exact replica of the high voltage waveforms under the condition of knowledge of the physical parameters of the instrumentation channel.

Introduction

Relaying, metering and disturbance recording uses a system of instrument transformers to scale the power system voltages and currents into instrumentation level voltages and currents. Standard instrumentation level voltages and currents are 67V or 115V and 5A respectively. These standards were established many years ago to accommodate the electromechanical relays. Today, the instrument transformers are still in use but

because modern relays, metering and disturbance recording operates at much lower voltages, it is necessary to apply another transformation from the previously defined standard voltages and currents to another set of standard voltages of 10V or 2V. This means that the modern instrumentation channel consists of typically two transformations and additional wiring and possibly burdens. Figure 1 illustrates typical instrumentation channels, a voltage channel and a current channel.

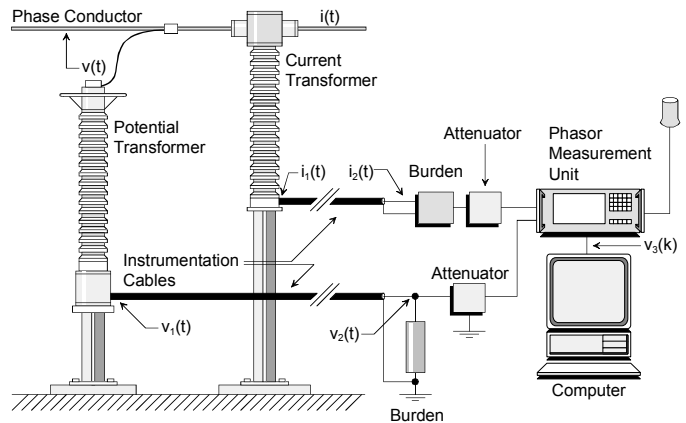


Figure 1. Typical Instrumentation Channel for DFR Data Collection

Note that each component of the instrumentation channel will introduce an error. Of importance is the net error introduced by all the components of the instrumentation channel. The overall error can be defined as follows. Let the voltage or current at the power system be:

$$v_a(t), \quad i_a(t)$$

An ideal instrumentation channel will generate a waveform at the output of the channel that will be an exact replica of the waveform at the power system. If

the nominal transformation ratio is k_v and k_i for the voltage and current instrumentation channels respectively, then the output of the ideal channels will be:

$$v_{ideal}(t) = k_v v_a(t), \quad i_{ideal}(t) = k_i i_a(t)$$

The error is defined as follows:

$$v_{error}(t) = v_{out}(t) - v_{ideal}(t), \quad i_{error}(t) = i_{out}(t) - i_{ideal}(t)$$

where the subscript “out” refers to the actual output of the instrumentation channel. The error waveform can be analyzed to provide the rms value of the error, the phase error, etc.

The instrumentation error can be computed by appropriate models of the entire instrumentation channel. It is important to note that some components may be subject to saturation (CTs and PTs) while other components may include resonant circuits with difficult to model behavior (CCVTs), see reference [6]. In this paper we present a new method for the simulation of the instrumentation channel. The method predicts with precision the instrumentation channel error. The method is also suitable for visualization of the operation of the instrumentation channel. Continuous visualization of the instrumentation channel errors provides a useful animation of the evolution of the errors. The paper presents the simulation method and describes the visualization and animation procedures of the instrumentation channel.

Instrumentation Channel Model

The analysis method presented here is a time domain simulation procedure that is based on quadratized models of all the components involved. Newton’s method is used to obtain the network solution. A brief description of the method is presented followed by the application of the method on the instrumentation channels.

Any device of the instrumentation channel (instrument transformer, cable, A/D converter, etc.) is described with a set of algebraic-differential-integral equations. These equations are obtained directly from the physical construction of the device. It is always possible to cast these equations in the following general form:

$$\begin{bmatrix} i \\ 0 \end{bmatrix} = \begin{bmatrix} f_1(\dot{v}, \dot{y}, v, y, u) \\ f_2(\dot{v}, \dot{y}, v, y, u) \end{bmatrix} \quad (1)$$

where i : vector of terminal currents,
 v : vector of terminal voltages,
 y : vector of device internal state variables
 u : vector of independent controls.

Note that this form includes two sets of equations, which are named *external equations* and *internal equations* respectively. The terminal currents appear only in the external equations. Similarly, the device states consist of two sets: *external states* (i.e. terminal voltages, $v(t)$) and *internal states* (i.e. $y(t)$). The set of equations (1) is consistent in the sense that the number of external states and the number of internal equations equals the number of external and internal equations respectively.

Note that equation (1) may contain linear and nonlinear terms. Equation (1) is quadratized, i.e. it is converted into a set of quadratic equations by introducing a series of intermediate variables and expressing the nonlinear components in terms of a series of quadratic terms. The resulting equations are integrated using a suitable numerical integration method. Assuming an integration time step h , the result of the integration is given with a second order equation of the form:

$$\begin{bmatrix} i(t) \\ 0 \end{bmatrix} = \begin{bmatrix} a_{11} & a_{12} \\ a_{21} & a_{22} \end{bmatrix} \begin{bmatrix} v(t) \\ y(t) \end{bmatrix} + \begin{bmatrix} (v^T(t), y^T(t))F_1 \\ (v^T(t), y^T(t))F_2 \\ \vdots \end{bmatrix} \begin{bmatrix} v(t) \\ y(t) \end{bmatrix} - \begin{bmatrix} b_1(t-h) \\ b_2(t-h) \end{bmatrix} \quad (2)$$

where: $b_1(t-h)$, $b_2(t-h)$ are past history functions.

The network solution is obtained by application of Kirchoff’s current law at each node of the system. This procedure results in the set of equations (3). To these equations, the internal equations are appended resulting to the following set of equations:

$$\sum_k A^k i^k(t) = I_{inj} \quad (3)$$

$$\text{internal equations of all devices} \quad (4)$$

where: I_{inj} is a vector of nodal current injections,

A^k is a component incidence matrix with:

$$A_{ij}^k = \begin{cases} 1, & \text{if node } j \text{ of component } k \text{ is connected to node } i \\ 0, & \text{otherwise} \end{cases}$$

Note that Equations (3) correspond one-to-one with the external system states while Equations (4) correspond one-to-one with the internal system states. The component k terminal voltage $v^k(t)$ is related to the nodal voltage vector $v(t)$ by:

$$v^k(t) = (A^k)^T v(t) \quad (5)$$

Upon substitution of device equations (2), the set of equations (3) and (4) become a set of quadratic equations:

$$Ax(t) + \begin{bmatrix} x^T(t)B_1(t)x(t) \\ x^T(t)B_2(t)x(t) \\ \vdots \end{bmatrix} - b(t-h) = 0 \quad (6)$$

where $x(t)$ is the vector of all external and internal system states.

Equations (6) are solved using Newton's method. Specifically, the solution is given by the following expression.

$$x^{v+1}(t) = x^v(t) - J^{-1}(Ax^v(t) + \begin{bmatrix} x^{vT}(t)B_1(t)x^v(t) \\ x^{vT}(t)B_2(t)x^v(t) \\ \vdots \end{bmatrix} - b(t-h)) \quad (7)$$

where: J is the jacobian matrix of equations (6) and $x^v(t)$ is the values of the state variables at the previous iteration.

The advantage of above procedure is that all equations are quadratic, i.e. both component model and network model. Newton's method provides an efficient and robust solution method for quadratic equations. This is very important when the system under simulation has highly nonlinear components such as the saturable core of an instrument transformer. It is important to state that the quadratized model of the components represent the exact nonlinear model of the device. For details of the quadratization procedure see reference [1].

Visualization and Animation

The instrumentation channel model provides the voltages and currents at any point of the instrumentation

channel at any time. It is possible to generate a snapshot of the voltages and currents at the various location of then instrumentation channel as well it is possible to compute metrics of the error between the actual voltages and currents and the ideal values. These metrics can be displayed on the same frame. As the simulation progresses, the visualization display is refreshed providing the sense of animation. This procedure will be demonstrated during the presentation of the paper.

Applications

In the next section, we present two applications: (a) one involving a current instrumentation channel and (b) another that involves a voltage instrumentation channel. For each one of these instrumentation channels, we present visualization results of the overall channel error for specific operating conditions. Several applications of the proposed instrumentation channel are presented here. The first example illustrates the visualization of CT saturation and its effects on recorded data accuracy. It is demonstrated that CT saturation is affected by control cable length as well as total burden on the CT. The second example illustrates the effect of instrumentation channel error on the operation of relays.

Example 1: Current Instrumentation Channel

A current instrumentation channel is illustrated in Figure 2. The channel consists of a CT (1200:5A), an 800 feet control cable, a burden of 0.1 ohm at the end of the control cable, and an A/D converter. For this particular instrumentation channel, the control cables are shielded cables. The shields are grounded at both ends of the cable. The cable itself is grounded only at the CT side of the circuit only. The parameters of the CT, the control cable and the A/D converter are illustrated in Figures 3, 4 and 5. Note that there is flexibility in selecting the parameters of the various components of the instrumentation channel. In addition to the model of the instrumentation channel, an "animator" model can be defined for the instrumentation channel. The parameters of this model are illustrated in Figure 6. This model is activated during simulation. Note that the animator data include the CT, the control cable, the burden, and the A/D converter. From this data, the animator "knows" the ideal transformation ratio at any point of the instrumentation channel. For example in the example of Figure 6, the ideal transformation ratio, between the

current of phase A of the 115 kV side to the terminal of the 0.1 ohm burden is 1200A to 0.5 Volts. Similarly, the ideal transformation can be defined for the output of the A/D converter.

During simulation, the waveform of the input to the instrumentation channel is displaced, superimposed on the waveforms at various point of the instrumentation channel, multiplied with the ideal transformation ratio at that point. In addition, the difference between any two waveform is also graphed and displayed. If the instrumentation channel was ideal, the various waveforms will be identical and the error waveform will be identically zero. The deviations are due to the nonideal characteristics of the instrumentation channel. Since the animation can be performed under any user defined scenarios, i.e. energization of a transformer, a fault, etc., this tool becomes a very useful investigative tool for determining the behavior of the instrumentation channel and the effects of the instrumentation channel errors on various relaying and disturbance recording applications.

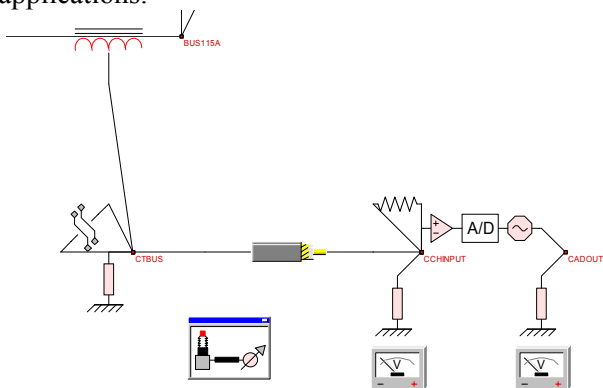


Figure 2. Computer Model of an Instrumentation Channel, CT Based

CT: 1200:5A, Phase A of 115 kV Bus		
Class	Error Class	5.0 (percent @ 20 pu)
	Voltage Class	200.0 Volts
Tap Selection	Tap Designation	X1-X2
	Primary Rating	1200.0 Amperes
	Secondary Rating	5.0 Amperes
	Coil Resistance	0.01 Ohms
	Leakage Reactance	0.012 Ohms
Device Supplying Primary Current: BUS115_A		
Circuit Number: 1		
Secondary: CTBUS_A, CTBUS_N		

Figure 3. Parameters of the CT - Instrumentation Channel of Figure 2.

RG-8 Control Cable, 800 ft. CT to Control House		Cancel
Number of Phases	<input type="radio"/> Single Phase <input checked="" type="radio"/> Two Phase <input type="radio"/> Three Phase	Existing Phase Conductors <input checked="" type="checkbox"/> Phase A <input checked="" type="checkbox"/> Phase B <input type="checkbox"/> Phase C
Parameters	Cable Type: CN_CABLE Cable Size: RG-8 Cable Configuration: URD2 Cable Length (miles): 0.152 Cable Length (feet): 800.0 Distance Between Grounds (feet): 800.0 Soil Resistivity (Ohm-Meters): 100.0 Ground Resistance (Ohms): 20.0	 Two Phase URD Cable, buried 3ft d
Bus Name, Side 1: CTBUS	Bus Name, Side 2: CCHINPUT	Circuit Number: 1

Figure 4. Parameters of the Control Cable - Instrumentation Channel of Figure 2.

A/D Converter Model, Configured for Current	
Input Attenuation Factor	5.0
Maximum A/D Converter Input Voltage	2.0 Volts
Maximum Output Voltage	10.0 Volts
Number of Bits	16.0
Sampling Rate	2880.0 samples per second
Conversion Time	350.0 microseconds

Figure 5. Parameters of the A/D Converter - Instrumentation Channel of Figure 2.

Phase A Current, 115 kV Bus, Instrumentation Channel Animation Model	
Device	115 kV Line, 9.6 miles, BUS115 to BUS115A
Nominal Value	1.2 kV or kA
Nodes	BUS115A_A, CACOUT_A
Nominal Value & Nodes	0.5 V, CCHINPUT_A, CCHINPUT_B
Buffer Size	4000
Nominal Value	0.707
Nodes	CACOUT_A, CACOUT_N

Figure 6. Parameters of the “Animator” Model - Instrumentation Channel of Figure 2.

Example 2: Voltage Instrumentation Channel

A voltage instrumentation channel is illustrated in Figure 7. The channel consists of a PT (66.4 kV:115 V),

an 800 feet control cable, a burden of 120.0 ohms at the end of the control cable, and an A/D converter. The control cable is a shielded cable grounded at both ends.

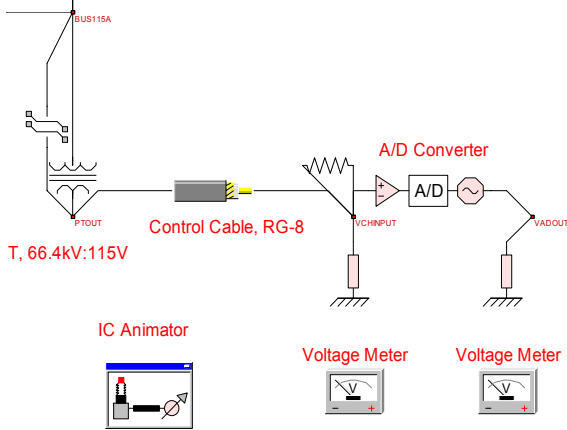


Figure 7. Computer Model of a Voltage Instrumentation Channel, PT Based

Single Phase Transformer		Cancel	Accept
PT: 66.4 kV/115 V, Phase A, 115 kV Bus			
Transformer Rating (kVA)	1.5	Tap Parameters	
Resistance (pu)	0.01	Tap Setting (pu)	1.0
Leakage Reactance (pu)	0.095	Minimum (pu)	1.0
Nominal Core Loss (pu)	0.005	Maximum (pu)	1.0
Nominal Magnetizing Current (pu)	0.005	Number of Taps	1
Primary Node Names BUS115A_A BUS115A_N		Secondary Node Names PTOUT_A PTOUT_N	
Primary kV Rating	66.4	Circuit Number	1
Secondary kV Rating	0.115		

Program WinIGS - Form IGS_M159

Figure 8. Parameters of the PT - Instrumentation Channel of Figure 7.

Analog to Digital Converter Model		Cancel	Accept
A/D Converter Model, Configured for Voltage			
Input Attenuation Factor	150.0		
Maximum A/D Converter Input Voltage	2.0	Volts	
Maximum Output Voltage	10.0	Volts	
Number of Bits	16.0		
Sampling Rate	2880.0	samples per second	
Conversion Time	350.0	microseconds	
VADOUT_A 300.00 Volts Max		VCHINPUT_A 1 Ohm	
VCHINPUT_N		VADOUT_N	
Attenuator		Circuit Number	
		1	

Program WinIGS - Form IGS_M138

Figure 9. Parameters of the A/D Converter - Instrumentation Channel of Figure 7.

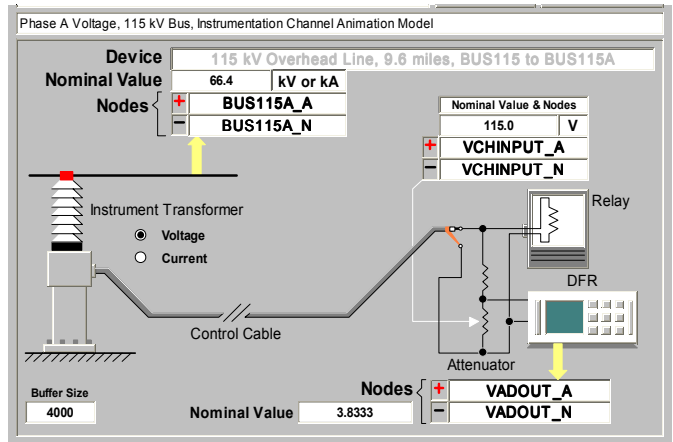


Figure 10. Parameters of the "Animator" Model - Instrumentation Channel of Figure 7.

The parameters of the PT and the A/D converter are illustrated in Figures 8 and 9, respectively. Note that there is flexibility in selecting the parameters of the various components of the instrumentation channel. In addition to the model of the instrumentation channel, an "animator" model can be defined for the instrumentation channel. The parameters of this model are illustrated in Figure 10. This model is activated during simulation. Note that the animator data include the PT, the control cable, the burden, and the A/D converter. From this data, the animator "knows" the ideal transformation ratio at any point of the instrumentation channel. For example in the case of Figure 10, the ideal transformation ratio, between the voltages of phase A of the 115 kV side and the terminal of the 120-ohm burden is 66400:115. Similarly, the ideal transformation can be defined for the output of the A/D converter.

Visualization and Animation of a Voltage Instrumentation Channel

The visualization and animation of any instrumentation channel is better explained with live demonstrations. During the presentation of the paper, live demonstrations of current and voltage instrumentation channels will be given. In this section we provide snapshots of the visualization and animation of a voltage instrumentation channel. The snapshot illustrates the response of the instrumentation channel during an event that combines two faults on the system: one fault results in a voltage sag at the input of the instrumentation channel. The fault is cleared in two cycles. This fault is followed by another fault that

causes a voltage swell at the input of the instrumentation channel. The fault again is cleared in two cycles. The simulated system is shown in Figure 11. It consists of a generator, a step-up transformer, a 115 kV line, another transformer and a load. Two snapshots are provided. The first snapshot shows the performance of the channel for one cycle before the first fault and one cycle after the first fault. This is illustrated in Figure 12. The top part of the figure illustrates the voltage at the input of the instrumentation channel, the voltage at the input of the A/D converter multiplied by the ideal transformation ratio and the voltage at the output of the A/D converter again multiplied by the ideal transformation ratio. The bottom part illustrates the error between at the input of the A/D converter as well as the error at the output of the A/D converter. Note the very high error during the fault transient. The second snapshot shows the performance of the channel for one cycle before the second fault and one cycle after the second fault. This is illustrated in Figure 13. Note that during this fault the voltage at the input of the instrumentation channel is experiencing a voltage swell. The error at the start of the fault transient is high but not as high as in the previous fault.

It is important to note that this tool permits the investigation of the impact of the various instrumentation channel parameters to the error of the measurement. For example, one can vary the control cable length, or use transient suppressers at the input of the A/D converter, etc. and observe the behavior of the error. Or, allow the instrument transformer to be saturated and observe the error. Another important issue is the transferred voltages to the instrumentation channel via the grounds. For this purpose, the substation ground should be added to the overall model. Again, some of these exercises will be demonstrated at the presentation of the paper.

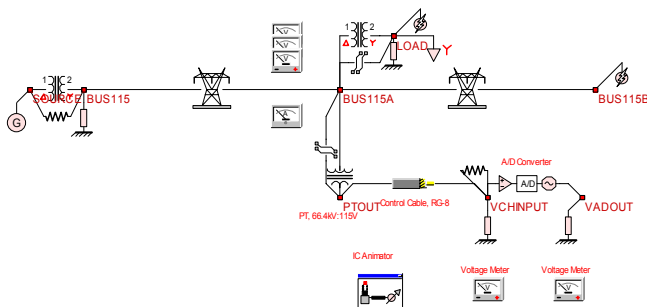


Figure 11. Example Power System for Visualization and Animation of an Instrumentation Channel

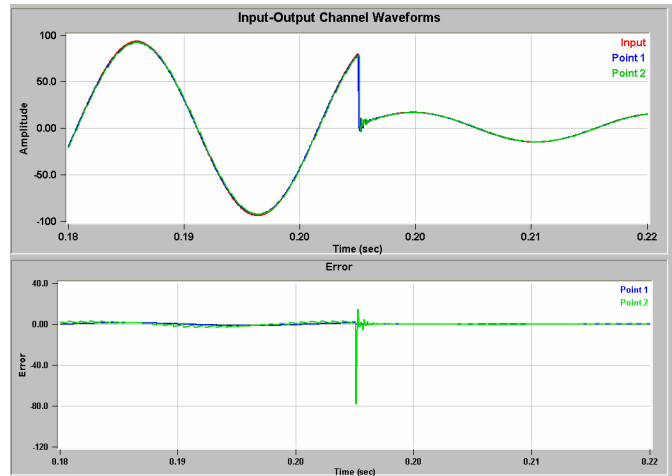


Figure 12. Snapshot of the Channel Performance One Cycle Before and One Cycle after the First Fault.

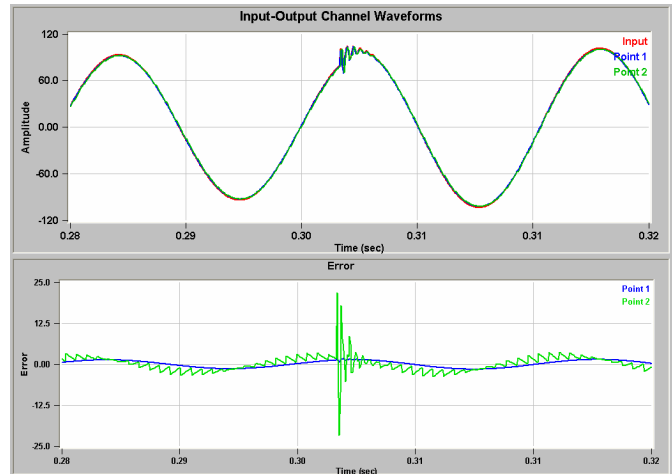


Figure 13. Snapshot of the Channel Performance One Cycle Before and One Cycle after the Second Fault.

Conclusions

This paper presented a method for the evaluation of the errors introduced by the various components of an instrumentation channel into the data collected by protective relays and disturbance recorders. There are operating conditions and power system disturbances that may result in excessive errors. In this case it will be necessary to correct these errors if the analysis of the data is to be meaningful. The inverse of the proposed method provides the basis for error correction. The usefulness of the proposed visualization and animation method is to realistically identify the various sources of

error. It can be a very useful tool for the design of power system instrumentation.

Acknowledgments

The work reported in this paper has been partially supported by the ONR Grant No. N00014-96-1-0926. This support is gratefully acknowledged.

References

1. A. P. Sakis Meliopoulos and George J. Cokkinides, "Virtual Power System Laboratories: Is the Technology Ready?", *Proceedings of the 2000 IEEE/PES Summer Meeting*, Seattle, WA, July 16-20, 2000.
2. A. P. Sakis Meliopoulos and George J. Cokkinides, 'A Virtual Environment for Protective Relaying Evaluation and Testing', *Proceedings of the 34th Annual Hawaii International Conference on System Sciences*, p. 44 (pp. 1-6), Wailea, Maui, Hawaii, January 3-6, 2001.
3. A. P. Sakis Meliopoulos, George J. Cokkinides, "Visualization and Animation of Protective Relays Operation From DFR Data", *Proceedings of the 2001 Georgia Tech Fault and Disturbance Analysis Conference*, Atlanta, Georgia, April 30-May 1, 2001.
4. A. P. Meliopoulos and J. F. Masson, "Modeling and Analysis of URD Cable Systems," *IEEE Transactions on Power Delivery*, vol. PWRD-5, no. 2, pp. 806-815, April 1990.
5. G. P. Christoforidis and A. P. Sakis Meliopoulos, "Effects of Modeling on the Accuracy of Harmonic Analysis," *IEEE Transactions on Power Delivery*, vol. 5, no. 3, pp.1598-1607, July 1990.
6. A. P. Meliopoulos, F. Zhang, S. Zelingher, G. Stillmam, G. J. Cokkinides, L. Coffeen, R. Burnett, J. McBride, 'Transmission Level Instrument Transformers and Transient Event Recorders Characterization for Harmonic Measurements,' *IEEE Transactions on Power Delivery*, Vol 8, No. 3, pp 1507-1517, July 1993.
7. A. Arifian, M. Ibrahim, S. Meliopoulos, and S. Zelingher, 'Optic Technology Monitors HV Bus', *Transmission and Distribution*, Vol. 49, No. 5, pp. 62-68, May 1997.
8. B. Fardanesh, S. Zelingher, A. P. Sakis Meliopoulos, G. Cokkinides and Jim Ingleson, 'Multifunctional Synchronized Measurement Network', *IEEE Computer Applications in Power*, Volume 11, Number 1, pp 26-30, January 1998.
9. T. K. Hamrita, B. S. Heck and A. P. Sakis Meliopoulos, 'On-Line Correction of Errors Introduced By Instrument Transformers In Transmission-Level Power Waveform Steady-State Measurements', *IEEE Transactions on Power Delivery*, Vol. 15, No. 4, pp 1116-1120, October 2000.

Biographies

A. P. Sakis Meliopoulos (M '76, SM '83, F '93) was born in Katerini, Greece, in 1949. He received the M.E. and E.E. diploma from the National Technical University of Athens, Greece, in 1972; the M.S.E.E. and Ph.D. degrees from the Georgia Institute of Technology in 1974 and 1976, respectively. In 1971, he worked for Western Electric in Atlanta, Georgia. In 1976, he joined the Faculty of Electrical Engineering, Georgia Institute of Technology, where he is presently a professor. He is active in teaching and research in the general areas of modeling, analysis, and control of power systems. He has made significant contributions to power system grounding, harmonics, and reliability assessment of power systems. He is the author of the books, *Power Systems Grounding and Transients*, Marcel Dekker, June 1988, *Lighning and Overvoltage Protection*, Section 27, Standard Handbook for Electrical Engineers, McGraw Hill, 1993, and the monograph, *Numerical Solution Methods of Algebraic Equations*, EPRI monograph series. Dr. Meliopoulos is a member of the Hellenic Society of Professional Engineering and the Sigma Xi.

George Cokkinides (M '85) was born in Athens, Greece, in 1955. He obtained the B.S., M.S., and Ph.D. degrees at the Georgia Institute of Technology in 1978, 1980, and 1985, respectively. From 1983 to 1985, he was a research engineer at the Georgia Tech Research Institute. Since 1985, he has been with the University of South Carolina where he is presently an Associate Professor of Electrical Engineering. His research interests include power system modeling and simulation, power electronics applications, power system harmonics, and measurement instrumentation. Dr. Cokkinides is a member of the IEEE/PES.